Analytical Biochemistry 554 (2018) 16–22

Contents lists available at ScienceDirect

Analytical Biochemistry

journal homepage: www.elsevier.com/locate/yabio

A target-triggered biosensing platform for detection of HBV DNA based on DNA walker and CHA

Feng Tao[a,1], Jie Fang[a,1], Yongcan Guo[b], Yiyi Tao[a], Xinle Han[a], Yuxin Hu[a], Jinjing Wang[c], Luyuan Li[a], Yulin Jian[a], Guoming Xie[a,*]

[a] Key Laboratory of Laboratory Medical Diagnostics, Ministry of Education, Department of Laboratory Medicine, Chongqing Medical University, Chongqing, 400016, PR China
[b] Clinical Laboratory of Traditional Chinese Medicine Hospital Affiliated to Southwest Medical University, Luzhou, 646000, PR China
[c] Department of Laboratory Medicine, Wenzhou Medical University, Wenzhou, 325000, PR China

ARTICLE INFO

Keywords:
Hepatitis B virus
DNA detection
DNA walker
Catalyzed hairpin assembly
Toehold-mediated strand displacement reaction

ABSTRACT

Hepatitis B virus (HBV), one of the causative agents of viral hepatitis, may lead to chronic hepatitis, cirrhosis, and liver cancer. In this work, we designed a sensitive and modular biosensing platform for detecting HBV DNA based on a DNA walker that hangs on to surfaces and a catalyst-triggered catalyzed hairpin assembly (CHA). In the presence of HBV DNA, strand displacement reaction between target and double-stranded complex caused the release of walker strand to trigger the DNA walker. Then, a catalyst was free to open the trapped hairpins to form a new double-strand complex, driving the CHA reaction. Thus, a powerful cascade amplification reaction realized in DNA walker and CHA based on toehold-mediated strand displacement reaction in this system. To achieve quantitative detection of HBV DNA, a fluorescent-quencher signaling pair was employed, the turn-on fluorescence provided an analytical signal. A wide detection range from 0.5 nM to 50 nM with a detection limit as low as 0.20 nM was reached on the condition of acceptable specificity and reproducibility. We could also further apply it to multiple different bioanalysis by changing adjustable elements. This reported biosensor opened a new avenue for sensitivity and modularity of DNA detection.

1. Introduction

Hepatitis B virus (HBV) is a blood-borne pathogen responsible for chronic hepatitis, cirrhosis, and liver cancer [1]. Currently, taking anti-HBV drugs is the most important and effective choice to inhibit viral replication. Anti-HBV drugs like lamivudine, have been widely used for the treatment of chronic hepatitis B (CHB) [2]. However, continuous drug therapy may become a thorny problem in clinical therapy due to gene mutation and selection of resistant strains. This requires that other measures should be taken to deal with HBV. The DNA of HBV, an important biomarker for HBV infection, can vary from a few to more than 109 copies/mL in serum, and it is usually detected in serum [3]. When infecting HBV, the concentration of HBV DNA increases in serum, providing a basis for early diagnosis of HBV. Therefore, DNA detection may become an important method for the early diagnosis of HBV.

The development of DNA detection technology has been the subject of intensive attentions for wide applications [4] owing to its important roles in pathogen analysis, genetic disorder diagnosis, and forensic tests [5]. More recently, several types of strategies have been developed to detect the HBV DNA, such as nanomaterial-based amplification [6–8], electrochemistry [3,9,10], fluorescence [11–14]. Despite the advantages and success in the detection of HBV DNA, these strategies suffer from either complex operation (synthesis of nanomaterial, preparation of biosensor) or lack of effective amplification system, which limit their further use in bioanalysis. Compared to above detection technologies, particularly in terms of fields of application, our system might be well suited to POC (point of care) use, which might be further enhanced by the use of magnetic particles, enabling omission of centrifugation steps and facilitating automation.

Signal amplification is a key component of molecular detection [15]. Molecular machines have previously been designed that are propelled by DNAzymes, protein enzymes and strand displacement [16], which can be adapted to signal-amplification. We have designed a simplified walker powered by Nb. BbvCI on the surface of microparticles, and apply it to the detection of HBV DNA. The walker consists of Nb. BbvCI, a walker strand (W) and a DNA coated on microparticles

* Corresponding author. Key Laboratory of Laboratory Medical Diagnostics of Education, Ministry of Education, Department of Laboratory Medicine, Chongqing Medical University, No. 1 Yi Xue Yuan Road, Chongqing, 400016, PR China.
E-mail addresses: xiegm059@foxmail.com, guomingxie@cqmu.edu.cn (G. Xie).
[1] These authors contributed equally.

https://doi.org/10.1016/j.ab.2018.05.024
Received 28 April 2018; Received in revised form 25 May 2018; Accepted 26 May 2018
Available online 30 May 2018
0003-2697/

(1 μm) surface that hybridizes with complementary W. W walkers upon the addition of Nb. BbvCI, which selectively hydrolyzes hybridized DNA but not single-stranded DNA (ssDNA). And the driving force for movement is derived from the free energy of binding new ssDNA [17]. In this walker, the specific signal transduction product is generated by the hydrolysis of the substrate by Nb. BbvCI. Thus, the walker will not be plagued by the movement of W that occurs during continuous amplification reaction and a corresponding loss in specificity due to the specificity of Nb. BbvCI. Hence, this walker has almost no meaningful background signal while continuing to move on the microparticles surface.

To obtain a strong signal in a short time, a nucleic acid circuit—the catalytic hairpin assembly (CHA) was employed in this system for further signal-amplification. This CHA circuit originally developed by Yin et al. has proven to be extraordinarily versatile [16,18]. In CHA, two hairpins are kinetically trapped, but in the presence of a single-stranded catalyst from enzyme-catalyzed product of walker, the single-stranded catalyst can undergo strand displacement reaction, leading to the formation of a double-stranded nucleic acid and recycling of the catalyst [16]. The CHA is powerful enough to achieve the signal amplification based on only strand displacement reaction. With the addition of signaling pair, the turn-on fluorescence provides an analytical signal for the detection of target.

In this work, two practical analytical features in this system should be considered. One is that the reaction must be efficient enough to achieve a high level of signal in a relatively short time. The other has to do with the possibility to optimize the design of the sensors to minimize background fluorescence and increase sensitivity.

Inspired by previous reports, we proposed a sensitive and modular biosensor for the detection of HBV DNA. Based on the negligible background and powerful amplification of DNA walker and CHA, the biosensor successfully achieved the quantitative detection of HBV DNA with low background and high sensitivity. Most importantly, this strategy could be modular to the application of detecting other targets by altering the corresponding DNA or aptamer sequence.

2. Materials and methods

2.1. Reagents and materials

All chemicals were purchased from Sigma-Aldrich Chemical Co. unless otherwise indicated. All oligonucleotides were synthesized by Sangon and the sequences were summarized in Table 1. Nb. BbvCI (5′-GC$^{\downarrow}$TGAGG-3′) and 10 × Smart® Buffer were purchased from New England Biolabs Inc. Microparticles (10 mg/mL, 1 μm) were purchased from Bangs Laboratories. Binding buffer (20 mM Tris, 1 M NaCl, 1 mM EDTA, 0.0005% TritonX-100, pH 7.4) was used as hybridization buffer. CST buffer (1 × CutSmart® Buffer, 0.01% TritonX-100, pH 7.9) was used as walker work buffer. All experiments were performed at room temperature (25 ± 2 °C) unless otherwise indicated.

2.2. Instrumentations

A Cary Eclipse Fluorescence spectrophotometer (Agilent, USA) was used to record fluorescence signals. An electrophoresis apparatus (DYY-6C, LIUYI, China) was used in electrophoresis experiment. An imaging system (Bio-Rad Laboratories, USA) was used to analyze gel image. The scanning electron microscope (SEM) (S-3000 N, Hitachi, Japan) was used to analyze the microparticles.

2.3. Preparation of W-Cp1-MP, Cp2-MP, H1 and H2

For the preparation of W-Cp1-MP, a portion of 5 μl of 20 μM Cp1 and W were incubated at 37 °C for 30 min with the same condition of volume and concentration. Then, streptavidin-coated microparticles (50 μl) from stock solution were washed once with 50 μl binding buffer by centrifuging the microparticles at 10,000 rpm for 3 min, followed by resuspension in 50 μl binding buffer. After that, a 10 μl volume of the W-Cp1 complex in binding buffer was added into the microparticles. After incubating for 15 min at 37 °C on a rotator, the sample was washed three times with 50 μl binding buffer to remove unbound complex by centrifuging the microparticles at 10,000 rpm for 3 min, followed by resuspension in 50 μl CST buffer. And the preparation of Cp2-MP was similar to above mentioned. A 10 μl volume of Cp2 in binding buffer was added into the resuspended microparticles. After incubation for 15 min at 37 °C on a rotator, the sample was washed three times with 50 μl binding buffer by centrifuging the microparticles at 10,000 rpm for 3 min, followed by resuspension in 50 μl CST buffer. In the CHA reaction, H1 and H2 in binding buffer were refolded by heating to 95 °C for 5 min, followed by slowly decreasing the temperature to 23 °C at a rate of 0.1 °C s^{-1}.

2.4. Detection of fluorescence

The detection of fluorescence intensity was performed under specific parameter conditions. To record the fluorescence endpoint measurements, the excitation wavelength was fixed at 480 nm and emission spectra were recorded between 500 and 600 nm. In the monitoring of real-time kinetics, the excitation wavelength and the emission wavelength was fixed at 480 nm and 520 nm, respectively. For all fluorescence detections, the width of excitation slit and the emission slit was 5 nm and 10 nm, respectively, all other parameters took the default.

2.5. Analysis of target

For detecting HBV DNA, a portion of 45 μl of HBV DNA in CST buffer was added to 5 μl of W-Cp1-MP in CST buffer, and incubating for 30 min at 37 °C on a rotator. Then decanting 44 μl of the supernatant by centrifuging the microparticles at 10,000 rpm for 3 min, followed by adding 5 μl of Cp2-MP into the supernatant. The walker continuously traveled on the microparticles surface at 37 °C when immediately adding 1 μl of Nb. BbvCI into above mixture. After incubating for

Table 1
Oligonucleotides designed in this study.

Oligonucleotides	Sequence (from 5′ to 3′)
HBV DNA (T)	TGGGAGGAGTTGGGGGAGGAGATTAGGTTAAAGGT
walker strand (W)	CCTCAGCAAAACCAAAAAACCAGTTGGGGGAGGAGAT
Capture probe 1 (Cp1)	Biotin - TTTTTTTTTTACCTTTAACCTAATCTCCTCCCCCAACTCCTCCCA
Capture probe 2 (Cp2)	Biotin - TTTTTTTTTTGGTTTTTTGGTTTTGC$^{\downarrow}$TGAGGCGACATCTAACCTAGCTCACTGAC ($^{\downarrow}$represents the identification point)
Hairpin 1 (H1)	GTCAGTGAGCTAGGTTAGATGTCGCCATGTGTAGACGACATCTAACCTAGCCCTTGTCATAGAGCAC
Hairpin 2 (H2)	AGATGTCGTCTACACATGGCGACATCTAACCTAGCCCATGTGTAGA
F	FAM - CGAGTGCTCTATGACAAGGGCTAGGTT
Q	CCCTTGTCATAGAGCACTCG - Dabcyl
1C-base mismatch target (T–1C-M)	TGGCAGGAGTTGGGGGAGGAGATTAGGTTAAAGGT
2C-base mismatch target (T–2C-M)	TGGCAGCAGTTGGGGGAGGAGATTAGGTTAAAGGT
3C-base mismatch target (T–3C-M)	TGGCAGCAGTTGGCGGAGGAGATTAGGTTAAAGGT

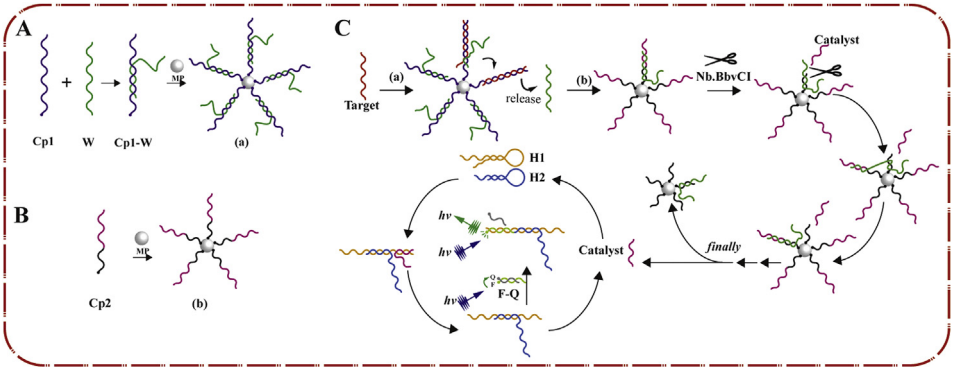

Scheme 1. Schematic of each detailed step and the sensing principle of the proposed DNA detection assay based on DNA walker and CHA.

180 min, the supernatant was obtained by centrifuging the microparticles at 10,000 rpm for 3 min. A portion of 20 μl of the supernatant was added into a 30 μl volume of the mixture H1 + H2 + F-Q (final volume: 50 μl; final concentration: H1, 0.2 μM; H2, 0.4 μM; F, 0.2 μM; Q, 0.4 μM). After incubating for 30 min at 37 °C in the dark, the fluorescence signal from the mixture was recorded in fluorescence spectrophotometer.

3. Results and discussion

3.1. Sensing strategy

The principle of this method is illustrated in Scheme 1. As shown, the capture probe 1 (Cp1) linked on particles surface were hybridized to the complementary W. In the presence of target (T, HBV DNA), T was hybridized with Cp1 via exposed toehold and strand displacement reaction, leading to the release of W. Then, W would hybridize with the complementary capture probe 2 (Cp2) coated on microparticles surface. The walker was triggered through the addition of Nb. BbvCI. While W traversed on microparticles surface, the single-stranded catalyst (C), which could trigger the CHA reaction, was released from Cp2. Then, C was hybridized to the toehold on H1 and opened the hairpin to expose an active ssDNA region via toehold-mediated strand displacement reaction. Then the toehold on H2 was hybridized to the active region and triggered branch migration, finally forming a tripartite complex, the H1:H2:C complex. As strand displacement proceeded, this complex resolved into the stable H1:H2 duplex according to thermodynamic interpretation. Displaced into freedom, C can then participate in subsequent reaction cycles. To achieve quantitative detection of HBV DNA, we employed a fluorescent-quencher signaling pair (F-Q) with a toehold which could bind a specific domain of F within the F-Q complex and initiate the branch migration reaction, resulting in separation between the fluorescent and quencher, and a fluorescence turn-on. Hence, this strategy has great potential for the detection of HBV DNA.

In this work, target HBV DNA was converted to a detectable, highly fluorescence signal in three steps. Firstly, a toehold-mediated strand displacement reaction was driven between target and complementary double-stranded nucleic acids, leading to the separation of W. In this step, The target was converted to W by 1:1 ratio. Then, W was hybridized to the complementary Cp2 coated on microparticles surface, followed by driving of the walker with the addition of Nb. BbvCI. As the walker step-to-step advanced, C was hydrolyzed and released from Cp2. A walker traversed on microparticle surface, it would cause the release of a large number of C. Finally, C triggered the CHA reaction via toehold-mediated strand displacement reaction. In CHA, C could participate in subsequent reaction cycles, resulting in the achievement of the cascade amplification. In the presence of the F-Q, target can be indirectly converted to the fluorescent turn-on.

In this strategy, efficiency and signal to noise ratio, the most crucial part, were directly decided by DNA walker and CHA. In walker, Nb. BbvCI drived the movement of walker. Although the use of Nb. BbvCI needed strict storage conditions and high requirements of the working environment, the machine which had been engineered to catalytic amplification with negligible background just consisting of Nb. BbvCI and complementary double-stranded nucleic acids. And in CHA, the circuit had almost zero background and a high catalytic efficiency by optimizing the design [13]. Admittedly, the walker, driven the movement by Nb. BbvCI, consumed a long time about 3 h. Time required for the enzymatic reaction could be reduced by increasing the preconcentrating effect of Nb. BbvCI and using the one of higher enzyme activity. For this restriction, we will further research the enzyme-driven walker machine and optimization conditions in the next experiment. Thence, our strategy worked efficiently based on double amplification system and had high signal to noise ratio due to negligible background on the whole.

3.2. Characteristics of this method

The SEM was used to characterize the microparticles. Fig. 1(A) and (B) provided the SEM images of microparticles. It can be observed that the microparticles were well dispersed homogenously with diameter size about 1 μm on average.

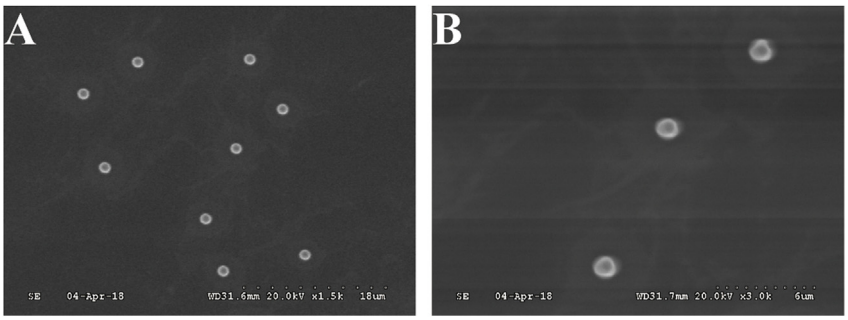

Fig. 1. SEM image of streptavidin-coated microparticles (1 μm).

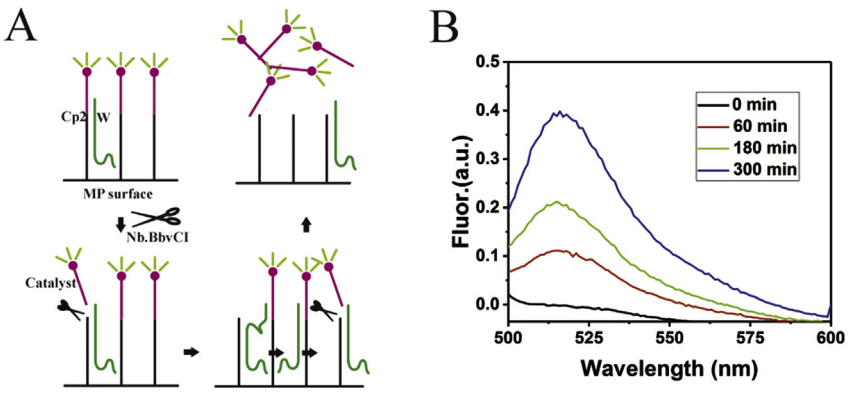

Fig. 2. (A) Schematic illustration of feasibility analysis of walker. (B) Fluorescence intensities of walker at t = 0 min (black line), 60 min (red line), 180 min (green line), 300 min (blue line), respectively. (For interpretation of the references to colour in this figure legend, the reader is referred to the Web version of this article.)

To evaluate the performance of walker, fluorescence was used for proving the movement of the walker. As shown in Fig. 2 (A), FAM-Cp2 coated on microparticles surface was hybridized with W, after adding Nb. BbvCI, the dsDNA was hydrolyzed and then C released from Cp2 due to instability. Then, through the toehold-mediated strand displacement reaction, C was hybridized to nearby Cp2 and participated in subsequent reaction cycles. Hence, many of FAM-C could be released into the supernatant, resulting in the fluorescent turn-on. In Fig. 2 (B), significant fluorescence enhancement was achieved over time, demonstrating that walker has good performance to be applied in the further experiment.

To verify the feasibility of CHA, we used agarose gel electrophoresis and fluorescence to prove the hybridization of hairpins with the catalysis of Cp2 (Here, we used Cp2 as the C). As shown in Fig. 3 (B), Lane 1 of the gel was loaded with DNA marker. Lane 2 and lane 3 was H1 and H2, respectively. When H1 and H2 were incubated for 120 min at room temperature, two bands were observed in lane 4 at the same location as lane 2 and lane 3 showed. Then, adding a small amount of Cp2 to H1 and H2, followed by incubating for 120 min at room temperature. As expected, a bright band in lane 5 was observed, indicating that Cp2 successfully triggered CHA. To monitor the assembly of H1 and H2 in real time, we used the fluorescent reporter construct F-Q. As shown in Fig. 3 (C), although mixture H1 + H2 (red line), mixture H1 + Cp2 (green line) and mixture H2 + Cp2 (black line) was respectively added to F-Q, no obvious fluorescence enhancement was observed. However, mixture H1 + H2 + Cp2 was added to F-Q, there was obvious change in fluorescence, showing that the presence of H1, H2, and Cp2 could make the CHA reaction work well. The fold-amplification of CHA was

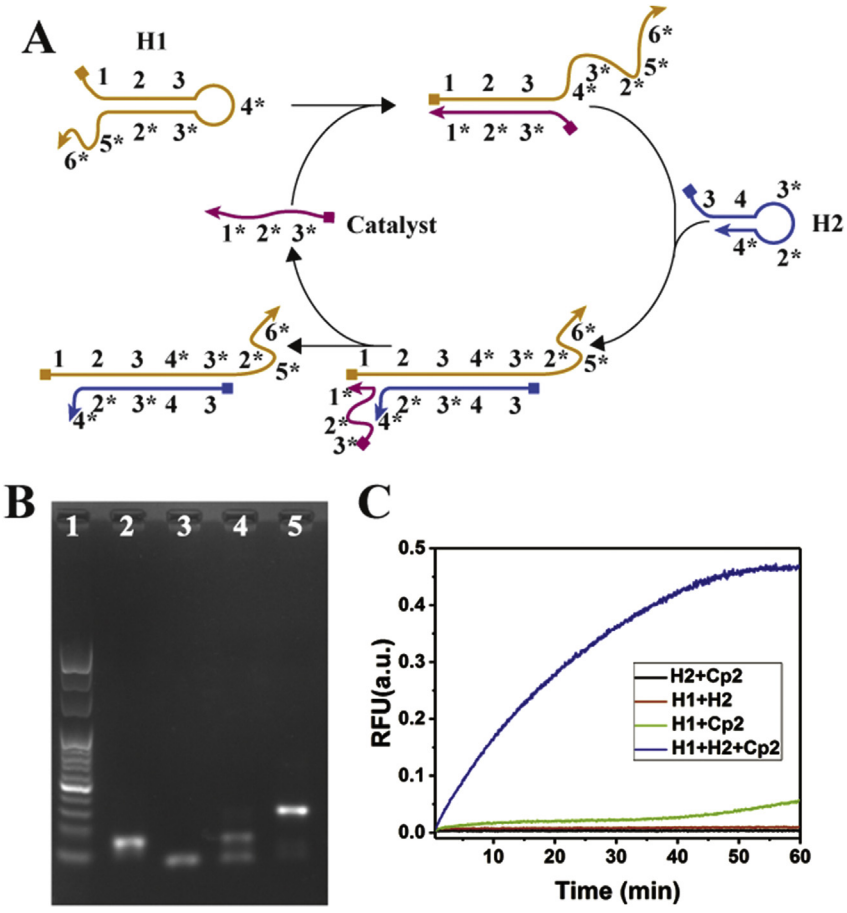

Fig. 3. (A) Schematic illustration of feasibility analysis of CHA. Squares and arrows drawn on DNA strands represent 5′ termini and 3′ termini, respectively. Domains are named by numbers and complementarity is denoted by asterisks. (B) The 3% agarose gel electrophoresis analysis under the different conditions: lane 1: DNA marker (2 μM); lane 2: H1 (2 μM); lane 3: H2 (2 μM); lane 4: H1 (2 μM) + H2 (2 μM); lane 5: H1 (2 μM) + H2 (2 μM) + Cp2 (0.1 μM). (C) Real-time kinetics of proof-of-concept for CHA.

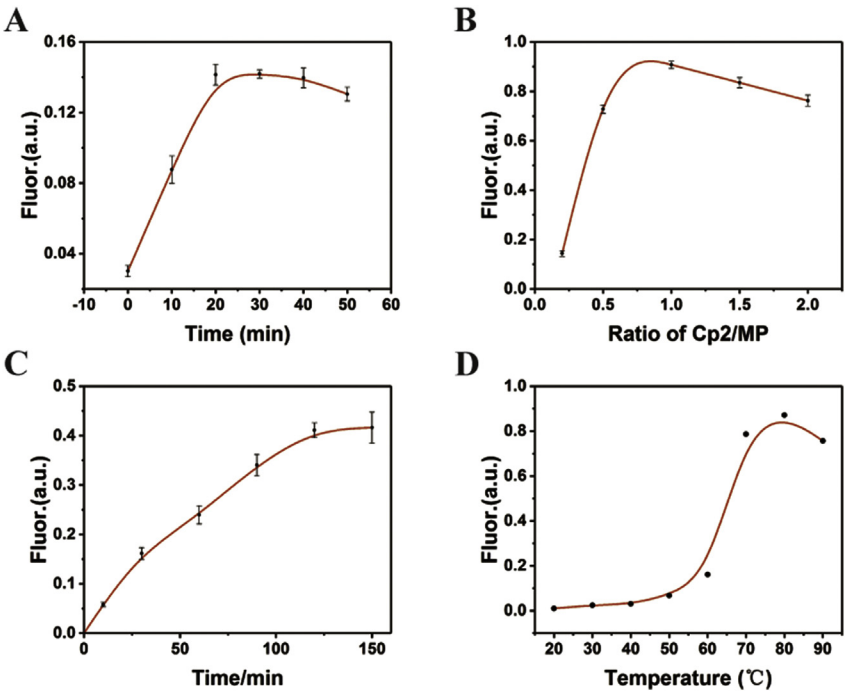

Fig. 4. Optimizations of experimental parameters: (A) the hybridization time between T and Cp1-W, (B) the ratio of Cp2 to microparticles, (C) the reaction time of CHA, (D) simulation curve of CHA without input C shows high stability in the range of temperatures of interest (from 20 to 40 °C). The target DNA concentration was 10 nM.

calculated as follows: $(F_{catalytic}\text{-}F_{non\text{-}catalytic})/(F_{non\text{-}H2}\text{-}F_{non\text{-}catalytic})$. Where $F_{catalytic}$, $F_{non\text{-}catalytic}$ and $F_{non\text{-}H2}$ represent the fluorescence of CHA, the fluorescence of CHA without Cp2 and the fluorescence of CHA without H2, respectively. And fold-amplification at t = 30 min is 18.75, demonstrating that CHA has high amplification efficiency. Hence, the CHA reaction was feasible.

3.3. Optimizations of the detection conditions

Detection conditions were the important factors that influenced analytical performances of the biosensor [19], such as incubation time, interface effect and temperature. The effect of incubation time of the strand displacement reaction between the target HBV DNA and Cp1-W on the microparticles surface was demonstrated in Fig. 4 (A). The fluorescence responses at different incubation times (0, 10, 20, 30, 40, and 50 min) were recorded. The fluorescence signal reached a plateau at t = 30 min. Hence, t = 30 min was considered as the optimum time.

As a signal amplification element, walker, one of the key section of the sensing process, is influenced by the ratio of Cp2 to microparticles (Cp2/MP) and the time of enzyme-catalytic reaction. We optimized the density of Cp2 on microparticles surface in this strategy. Fig. 4 (B) showed that the fluorescence signal increased with the increasing of ratio of Cp2/MP within limit of about 0.75 and then gradually decreased. And as shown in Fig. S1, negative control indicated that the background also changed with the same trend. It was possible that the stability of DNA sphere was weakened owing to the high density. DNA polyanion had high colloidal stability in solution [20], however, DNA sphere increased the local concentration of DNA, which in turn enhanced the mutual repulsion between DNA molecules, resulting in high background. While the ratio of Cp2/MP was 0.2, the highest signal to noise ratio was obtained. Hence, 0.2 was considered as the optimum ratio of Cp2/MP. We also optimized the time of enzyme-catalytic reaction. As shown in Fig. S2,the signal of enzyme-catalytic reaction was recorded at different incubation times (60, 120, 180, 240, and 300 min). Taking into account the sensitivity and efficiency of detection, t = 180 min was considered as the optimum time of walker. Meanwhile, we could observe that the fluorescence signal did not reach a plateau at t = 300 min. To calculate the average rate of the walker (F/min), we measured the fluorescence intensities from t = 60 min to t = 300 min. The difference of fluorescence intensity at t = 60 min and t = 300 min was divided by 240 min to obtain the average rate (F/min). The reaction rate of walker (2.90 F/min) was slower than that we expected. This is likely due to the low density of Cp2 on microparticles surface, affecting the hybridization of W and Cp2, thus influencing the movement of walker.

The sensing process was also influenced by the assembly time and the stability of CHA. As shown in Fig. 4 (C), the signal maintained increasing in the range from 0 to 150 min. At t = 30 min, the signal could provide the sensitivity and efficiency of detection in the sensing process. Thus, t = 30 min was chosen as the optimal assembly time for CHA. The stability of CHA was verified in our experiment and was shown in Fig. 4 (D). We placed CHA composition without input C at different temperatures (from 20 to 90 °C) and incubated for 30 min, followed by observing the change of fluorescence signal. As we can see, the CHA was stable from 20 to 40 °C. To reduce the time required for the CHA reaction and consider the convenience of application in bioanalysis, we regard 37 °C as the optimum temperature in this study.

3.4. Sensitivity

Fig. S3 (A) and (B) showed the scan and simulation curve of the fluorescence signal variation versus the target concentration (0, 0.05, 0.10, 0.50, 1, 10, 25, 50, 75, 125, 150 nM) under the optimum experimental conditions, respectively. As shown in Fig. 5(A) and (B). The calibration curve showed a good linear relationship between the fluorescence intensity and concentration ranging from 0.5 nM to 50 nM. The HBV DNA concentration was calculated according to the equation: $Y = 7.4632C + 30.1359$ ($R^2 = 0.9958$), where Y and C represent the fluorescence signal intensity (a.u.) and the concentration of the target DNA (nM), respectively. And the detection limit could be estimated as 0.20 nM on the basis of 3 S/slope (S is the standard deviation of blank samples), which was comparable or even better than some of other reported methods, as shown in Table S1. Such a considerable detection limit of our sensing strategy can be primarily attributed to the powerful cascade amplification reaction in DNA walker and CHA based on toehold-mediated strand displacement reaction in this system. In addition, with wide detection range, the biosensor has more options for different concentrations of target.

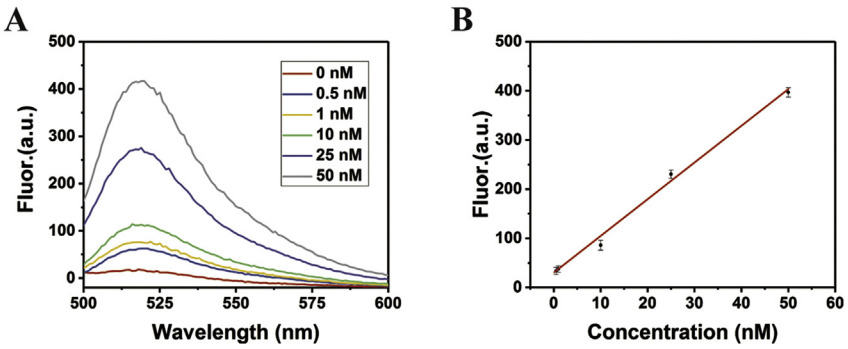

Fig. 5. (A) Fluorescence intensities of target concentration 0 nM (red line); 0.5 nM (blue line); 1 nM (yellow line); 10 nM (green line); 25 nM (purple line); 50 nM (gray line), respectively. (B) The calibration curve between the concentration of the target DNA and fluorescence signal. All error bars represent standard deviations of the measurements (n = 3). (For interpretation of the references to colour in this figure legend, the reader is referred to the Web version of this article.)

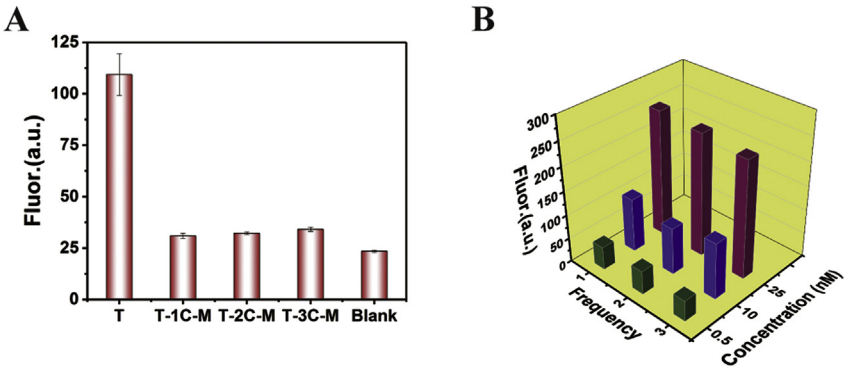

Fig. 6. (A) Specificity investigation against the target DNA (T), single base mismatch DNA (T-1C-M), two bases mismatch DNA (T-2C-M), three bases mismatch DNA (T-3C-M), and hybridization buffer (blank). All detected target concentration was 10 nM. (B) Reproducibility of the proposed sensing strategy in different concentration.

3.5. Specificity and reproducibility

In terms of the gene, the very tiny change of gene physicochemical property resulting from the point mutation adds great difficulty to its detection, so the point mutation discrimination ability becomes one of the most important performance parameters for gene detection technologies [21,22]. To illustrate the discrimination ability for the point mutation, we tested three types of oligonucleotides with 1, 2, 3 base-mismatch, respectively. The concentration of target was 10 nM each. As Fig. 6 (A) showed, compared with blank, no remarkable change was observed toward the tested oligonucleotides. These results showed that this strategy had high specificity.

Reproducibility of this biosensor was further tested and shown in Fig. 6 (B). Different concentrations of the target (0.5, 10, 25 nM) were detected with the same process and the relative standard deviation was 6.48%, 9.31%, and 3.41%, respectively. Hence, it could be concluded that the DNA biosensor had satisfactory reproducibility.

4. Conclusion

In summary, a novel fluorescence biosensor for DNA detection based on DNA walker that hangs on to surfaces and CHA was successfully fabricated. The reported biosensor provided low background and high sensitivity, which changed linearly in target concentration ranging from 0.50 to 50 nM with a low detection limit of 0.20 nM. With the satisfactory specificity and reproducibility, the biosensor could identify single base mutation. Meanwhile, we noted that this strategy could be modular to the application of detecting different targets by altering the corresponding DNA or aptamer sequence. With these excellent properties, our biosensor may have great potential for genetic detection of pathogens, human disease susceptibility or related genes.

Declarations of interest

None.

Acknowledgment

This work was financially supported by National Natural Science Foundation of China (No. 81672112).

Appendix A. Supplementary data

Supplementary data related to this article can be found at http://dx.doi.org/10.1016/j.ab.2018.05.024.

References

[1] G. Choijilsuren, R.S. Jhou, S.F. Chou, C.J. Chang, H.I. Yang, Y.Y. Chen, W.L. Chuang, M.L. Yu, C. Shih, Heparin at physiological concentration can enhance PEG-free in vitro infection with human hepatitis B virus, Sci. Rep. 7 (2017) 14461.
[2] X. Wang, X. Lou, Y. Wang, Q. Guo, Z. Fang, X. Zhong, H. Mao, Q. Jin, L. Wu, H. Zhao, J. Zhao, QDs-DNA nanosensor for the detection of hepatitis B virus DNA and the single-base mutants, Biosens. Bioelectron. 25 (2010) 1934–1940.
[3] X. Li, K. Scida, R.M. Crooks, Detection of hepatitis B virus DNA with a paper electrochemical sensor, Anal. Chem. 87 (2015) 9009–9015.
[4] M. Shariati, The field effect transistor DNA biosensor based on ITO nanowires in label-free hepatitis B virus detecting compatible with CMOS technology, Biosens. Bioelectron. 105 (2018) 58–64.
[5] Y. Xiang, Y. Lu, Using commercially available personal glucose meters for portable quantification of DNA, Anal. Chem. 84 (2012) 1975–1980.
[6] M.M. Gong, R. Nosrati, M.C. San Gabriel, A. Zini, D. Sinton, Direct DNA analysis with paper-based ion concentration polarization, J. Am. Chem. Soc. 137 (2015) 13913–13919.
[7] X. Mao, S. Liu, C. Yang, F. Liu, K. Wang, G. Chen, Colorimetric detection of hepatitis B virus (HBV) DNA based on DNA-templated copper nanoclusters, Anal. Chim. Acta 909 (2016) 101–108.
[8] Y. Li, S. Liu, Q. Deng, L. Ling, A sensitive colorimetric DNA biosensor for specific detection of the HBV gene based on silver-coated glass slide and G-quadruplex-hemin DNAzyme, J. Med. Virol. 90 (2018) 699–705.
[9] A.C. Honorato Castro, E.G. França, L.F. de Paula, M.M.C.N. Soares, L.R. Goulart, J.M. Madurro, A.G. Brito-Madurro, Preparation of genosensor for detection of specific DNA sequence of the hepatitis B virus, Appl. Surf. Sci. 314 (2014) 273–279.
[10] J. Zheng, C. Chen, X. Wang, F. Zhang, P. He, A sequence-specific DNA sensor for Hepatitis B virus diagnostics based on the host–guest recognition, Sensor. Actuator. B Chem. 199 (2014) 168–174.
[11] H. Zhu, F. Lu, X.C. Wu, J.J. Zhu, An upconversion fluorescent resonant energy transfer biosensor for hepatitis B virus (HBV) DNA hybridization detection, Analyst 140 (2015) 7622–7628.
[12] J. Chen, Q. Chen, C. Gao, M. Zhang, B. Qin, H. Qiu, A SiO2 NP–DNA/silver

nanocluster sandwich structure-enhanced fluorescence polarization biosensor for amplified detection of hepatitis B virus DNA, J. Mater. Chem. B 3 (2015) 964–967.
[13] L. Chen, L. Song, Y. Zhang, P. Wang, Z. Xiao, Y. Guo, F. Cao, Nitrogen and Sulfur Codoped, Reduced graphene oxide as a general platform for rapid and sensitive fluorescent detection of biological species, ACS Appl. Mater. Interfaces 8 (2016) 11255–11261.
[14] C. Zhang, Y. Chen, X. Liang, G. Zhang, H. Ma, L. Nie, Y. Wang, Detection of hepatitis B virus M204I mutation by quantum dot-labeled DNA probe, Sensors 17 (2017).
[15] B. Li, A.D. Ellington, X. Chen, Rational, modular adaptation of enzyme-free DNA circuits to multiple detection methods, Nucleic Acids Res. 39 (2011) e110.
[16] C. Jung, P.B. Allen, A.D. Ellington, A stochastic DNA walker that traverses a microparticle surface, Nat. Nanotechnol. 11 (2016) 157–163.
[17] P. Yin, H.M. Choi, C.R. Calvert, N.A. Pierce, Programming biomolecular self-assembly pathways, Nature 451 (2008) 318–322.
[18] K. Yehl, A. Mugler, S. Vivek, Y. Liu, Y. Zhang, M. Fan, E.R. Weeks, K. Salaita, High-speed DNA-based rolling motors powered by RNase H, Nat. Nanotechnol. 11 (2016) 184–190.
[19] X. Chen, L. Wang, S. Sheng, T. Wang, J. Yang, G. Xie, W. Feng, Coupling a universal DNA circuit with graphene sheets/polyaniline/AuNPs nanocomposites for the detection of BCR/ABL fusion gene, Anal. Chim. Acta 889 (2015) 90–97.
[20] C. Fernandez-Solis, Y. Kuroda, A. Zinchenko, S. Murata, Uptake of aromatic compounds by DNA: toward the environmental application of DNA for cleaning water, Colloids Surfaces B Biointerfaces 129 (2015) 146–153.
[21] F. Li, Y. Xu, X. Yu, Z. Yu, X. He, H. Ji, J. Dong, Y. Song, H. Yan, G. Zhang, A "signal on" protection-displacement-hybridization-based electrochemical hepatitis B virus gene sequence sensor with high sensitivity and peculiar adjustable specificity, Biosens. Bioelectron. 82 (2016) 212–216.
[22] K. Chang, S. Deng, M. Chen, Novel biosensing methodologies for improving the detection of single nucleotide polymorphism, Biosens. Bioelectron. 66 (2015) 297–307.